GEOPHYSICAL RESEARCH LETTERS, VOL. 35, L03202, doi:10.1029/2007GL031957, 2008

Implications of shear heating and fracture zones for ridge formation on Europa

Lijie Han[1] and Adam P. Showman[2]

Received 11 September 2007; revised 19 December 2007; accepted 4 January 2008; published 7 February 2008.

[1] We present 2D and 3D numerical simulations of convection to test the role of shear heating and fracture zones on Europan ridge formation. Our simulations show that a pre-existing fracture zone promotes upwelling and lithospheric thinning, leading to topographic uplift of 50 m. Shear heating also promotes lithospheric thinning and buoyant ascent, producing a ridge-like feature with topography up to 120 m. Topography remains linear along strike even under the influence of heterogeneous 3D convection within the ice shell. Although the central trough is not reproduced in the simulations, our results support the idea that shear heating can produce ridge-like structures on Europa. **Citation:** Han, L., and A. P. Showman (2008), Implications of shear heating and fracture zones for ridge formation on Europa, *Geophys. Res. Lett.*, *35*, L03202, doi:10.1029/2007GL031957.

1. Introduction

[2] Ridges are ubiquitous on Europa. Typically, ridges are ~100–300 m in height, a few kilometers in width, and contain a central trough [*Head and Pappalardo*, 1999]. Many ridge-formation scenarios have been suggested [*Pappalardo et al.*, 1999; *Greeley et al.*, 2004]. These scenarios include tidal "squeezing" of slushy ice onto the surface through existing fractures [*Greenberg et al.*, 1998]; build-up of volcanic debris along the fractures [*Kadel et al.*, 1998]; compressive upwarping [*Sullivan et al.*, 1998]; upwarp resulting from buoyant ascent of linear diapirs through pre-existing fractures [*Head and Pappalardo*, 1999]; injection of melt into dikes in Europa's ice lithosphere, which would cause upward deformation [*Melosh and Turtle*, 2004]; and frictional heating along fractures, which causes a temperature increase and leads to buoyant uplift along the fracture [*Gaidos and Nimmo*, 2000; *Nimmo and Gaidos*, 2002].

[3] *Nimmo and Gaidos* [2002] demonstrated that frictional heating can indeed localize along tidally sheared faults. Simple buoyancy arguments suggest that these temperature increases can lead to flexural uplift of up to ~100 m, which is encouragingly close to typical ridge heights on Europa. However, existing studies of shear heating have not considered advection within the shell, so they have been unable to determine the morphology of uplift and the detailed subsurface deformation in response to shear heating. Even if the ice shell is not convecting, deformation will occur in response to the focused heating, and in the most extreme case the heating could trigger linear diapirs [*Head et al.*, 1999]. Moreover, convection may occur in Europa's ice shell [*McKinnon*, 1999; *Tobie et al.*, 2003; *Showman and Han*, 2004, 2005; *Barr et al.*, 2004; *Mitri and Showman*, 2005] and this could alter the response of the ice shell to shear heating. In particular, it is unclear whether a ridge that is uniform along-strike can form in the presence of heterogeneous, 3D convection in the underlying ice. To rigorously determine whether shear heating can cause ridge formation under Europan conditions, a full fluid-dynamical model including advection of heat is required.

[4] Here, we present two- and three-dimensional numerical simulations of convection to test the role of fracture zones and shear heating on Europan ridge formation. These preliminary simulations do not consider compositional (salinity) effects.

2. Model and Methods

[5] We used the finite-element codes ConMan [*King et al.*, 1990] and CitCom [*Moresi et al.*, 1996] to solve the equations governing thermal convection in Europa's ice shell in two- and three- dimensional Cartesian geometry. In 2D, the aspect ratio of length and depth is 3:1, and the resolution is 300 × 100 elements. In 3D, the aspect ratio of length, depth, and width is 3:1:1, and the resolution is 301 × 101 × 65 elements. We ran some 2D test cases with up to 400 elements in the vertical, which show that our nominal resolutions are adequate to characterize the basic convective behavior and surface topography. The velocity boundary conditions are reflective or periodic on the sides and free-slip on the top and bottom. The temperature boundary condition at the bottom is fixed (270 K), as required by the underlying ocean, and the top is held at 95 K. The initial temperature increases linearly from the top to the bottom, with a small disturbance (of amplitude 2.7 K) to trigger convection. Tidal heating is included in the simulations as that of *Showman and Han* [2004]. Temperature-dependent viscosity follows the relation

$$\eta = \eta_0 \exp\left[A\left(\frac{T_m}{T} - 1\right)\right] \tag{1}$$

where T is temperature, T_m = 270 K, and η_0 is the viscosity at 270 K. An activation energy of 20–60 kJ mol^{-1} is used [*Goldsby and Kohlstedt*, 2001], corresponding to values of A ranging from 9–26, which implies viscosity contrasts of ~10^7 to 6 × 10^{20}. Varying this parameter allows us to investigate the extent to which the stiffness of the surface ice influences the behavior.

[1]Planetary Science Institute, Tucson, Arizona, USA.
[2]Department of Planetary Sciences, Lunar and Planetary Laboratory, University of Arizona, Tucson, Arizona, USA.

0094-8276/08/2007GL031957$05.00

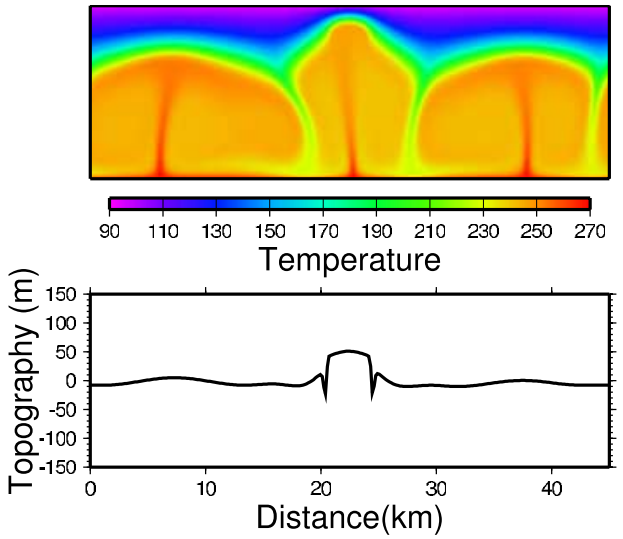

Figure 1. (top) Temperature and (bottom) dynamic topography from a model in a domain 45 km wide and 15 km deep. This model includes a weak zone 4 km wide but no shear heating. The Rayleigh number is 1.8×10^7, depth of weak zone is 5 km, and activation energy is 20 kJ/mol.

[6] We run two sets of 2D simulations. For the first set of simulations, we impose a narrow (few km-wide) weak zone extending vertically downward from the surface to the base of the lithosphere (i.e., base of the stagnant lid). The weak zone is implemented by simply lowering the viscosity in the weak zone by an order of magnitude relative to the surrounding regions. This is a standard method for representing faults in ridges and subduction zones in the Earth mantle-convection community [*Zhong et al.*, 1998]. No shear heating is included in this first set. These simulations are performed to test the influence of weak zones (fracture zones) on fluid flow and surface topography.

[7] For the second set of simulations, we impose a narrow, linear strip of tidal heating extending vertically downward from the surface into the interior. *Nimmo and Gaidos* [2002] showed that shear heating maximizes at the bottom of brittle layer and decreases with distance away from shear zone and depth inside the ductile layer. Here, we crudely specify the shear heating with a functional form

$$s = s_0(z) \exp\left[-\frac{(x - x_0)^2}{\sigma_x^2}\right] \quad (2)$$

where $s_0(z)$ is a specified depth dependence (large at the surface and diminishing linearly downward to zero at a depth of 3–4 km), σ_x is the specified half width of the heating zone (less than 1 km), z is height, and x is horizontal distance. We assume that $s_0(z)$ is independent of time. In equation 2, x_0 is the horizontal central location of the shear heating, which is placed at the half-way point of the domain. The goal of these simulations is to investigate the influence of shear heating on the fluid flow and surface topography.

[8] We treat the magnitude of shear heating as a free parameter guided by the results of *Nimmo and Gaidos* [2002]. The heat generated within the shear zone per unit area perpendicular to the shear zone is $H = \mu_f \rho g u d$, where μ_f is the friction coefficient, ρ is density, g gravity, d depth, and u the shear velocity associated with diurnal tidal flexing. Adopting $\mu_f = 0.1$, $\rho = 920$ kg m^{-3}, and $g = 1.3$ m sec^{-2}, this yields peak values up to $H \approx 0.2\,(u/10^{-6}\ \text{m sec}^{-1})$ W m^{-2} at a depth of ~2 km [*Nimmo and Gaidos*, 2002], which is a probable thickness for the brittle layer. Given our gaussian formulation (Equation 2), $s_0(z)$ should then reach a peak value of $H/(\sqrt{\pi}\sigma_x) \approx 0.1\sigma_x^{-1}\,(u/10^{-6}\ \text{m sec}^{-1})$ W m^{-3}. For a velocity of $u = 10^{-6}$ m sec^{-1} appropriate to diurnal tidal flexing [*Nimmo and Gaidos*, 2002], and $\sigma_x = 0.2$–1 km, this yields a maximum s_0 value in the range 1–5×10^{-4} W m^{-3}. And order-of-magnitude estimates from *Preblich et al.* [2007], based on their finite-element models of tidal walking, suggest that the peak heating at tidally flexed fractures reaches $\sim 1 \times 10^{-4}$ W m^{-3}. We explore values in this range.

3. Results

[9] Figure 1 displays the results from a 2D model including a weak zone but no shear heating. The weak zone, which represents an existing fracture region, was placed at the halfway point of the domain (x = 22.5 km), had a width of 4 km, and extended vertically from the surface to a depth of 5 km. The calculation domain was 45 km wide and 15 km deep. In the simulation, the weak zone modulates the convective structure, leading to a lithosphere at the weak zone that is much thinner than in the surrounding regions. The topography at the weak zone becomes uplifted by up to ~50 m, but this is much smaller than observed ridge heights of 100–300 m. This simulation shows that an upwelling plume (or diapir) may exist under weak zones (fracture zones), but it is hard to explain the full topography of observed ridges without invoking the buoyancy from locally enhanced (tidal or shear) heating. In cases where the weak zone does not penetrate the stagnant lid, or when a larger activation energy of 60 kJ mol^{-1} is used, the surface topography is even weaker than shown in Figure 1.

[10] Figure 2 displays the results from a 2D model with shear heating (following equation 2) but no weak zone. The shear heating zone extends vertically from the surface to 4 km depth, has a half width σ_x = 0.4 km and maximum heating rate of 5×10^{-4} W m^{-3}. The calculation domain is 60 km wide and 20 km deep. An activation energy of 60 kJ mol^{-1} is used in the model. In the simulation, the stagnant lid becomes greatly thinned at the location of the shear heating. The resulting topography (Figure 2) reaches 120 m in height, comparable to that estimated to order-of-magnitude by *Nimmo and Gaidos* [2002] and to the observed height of typical Europan ridges (up to 100–300 m). Analogous simulations performed with activation energies of 20 and 30 kJ mol^{-1} show that the topography is relatively insensitive to the activation energy. Interestingly, the topographic morphology broadly resembles that of a Europan ridge, including shallow marginal troughs on either side of the ridge, although these sometimes disappear as the evolution proceeds. If the heating continues indefinitely, the ridges approach a steady-state structure after 10^6 years, with a ~4–6 km-wide and ~50–60 m-tall ridge superposed on a low-amplitude regional swell 10–20 km across. However, the central trough is not reproduced. Despite this deficiency,

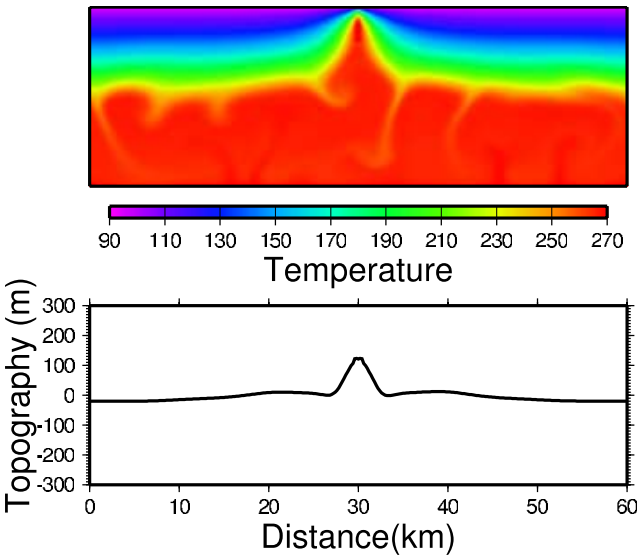

Figure 2. (top) Temperature and (bottom) dynamic topography from a model in a domain 60 km wide and 20 km deep. This model includes shear heating but no weak zone. The Rayleigh number is 4.2×10^7, activation energy is 60 kJ/mol, and depth of shear heating is 4 km. Shear heating s(z) decays linearly with depth. s_0 (maximum shear heating rate) is 5×10^{-4} W m^{-3}, and σ_x (half width of the shear heating zone) is 0.4 km.

our models lend support to the idea that shear heating can produce ridge-like structures on Europa.

[11] Ridge morphology differs slightly as σ_x is varied. In the steady state, the ridges crests are generally flat and the total ridge width tends to be 4–6 km for σ_x = 0.4 km but reaches 6–10 km for σ_x = 1 km.

[12] Our simulations neglect elasticity. To estimate the impact of elasticity on the topography, we use standard relations for the flexural uplift caused by a low-density structure beneath an elastic lithosphere [e.g., *Nimmo and Manga*, 2002]. We adopt a radius $r \sim 3$ km for the heated region, a temperature constant ~80 K between this region and the surroundings (see Figure 2), and a thermal expansivity $\alpha \sim 1.6 \times 10^{-4}$ K^{-1} for ice. Adopting an elastic thickness of 200 m and a Young's modulus of 6×10^9 [see *Billings and Kattenhorn*, 2005, Table 2] implies that the elasticity would decrease the topography by ~30%.

[13] We explored three different maximum shear heating values, $s_0(0)$, of 1×10^{-4} Wm^{-3}, 5×10^{-4} Wm^{-3}, and 1×10^{-3} Wm^{-3} to test the influence of shear heating magnitude on Europan ridge formation. Our results show that when the shear heating value is less than 1×10^{-4} Wm^{-3}, no ridge-like topography forms in the simulations. The temperature increases at the location of shear heating zone, but it is too weak to produce significant surface topography. Ridge-like features up to 100–120 m are obtained when the shear heating ($s_0(0)$) lies between 5×10^{-4} and 1×10^{-3} Wm^{-3}. This suggests that shear velocity at the fracture zone should be at least ~10^{-6} m sec^{-1} for shear heating to produce ridges.

[14] To investigate the influence of heterogeneous convection on Europa's ridge formation, we ran a few 3D simulations using the finite-element code CitCom. We impose an irregular initial temperature disturbance in the lower part of the calculation domain to break the symmetry along-strike. Figures 3 and 4 depict temperature and surface topography results from 3D models with shear heating. Both simulations are run in a domain 15 km deep. Shear heating is included along the strike of fracture zone, with a half width (σ_x) of 0.4 km and depth of 3 km. We implement an activation energy of 20 kJ mol^{-1} in both simulations. Figure 3 displays results from a model with melting-point viscosity of 10^{14} Pa s, and Figure 4 displays results from a model with melting-point viscosity of 10^{13} Pa s. Despite the strongly heterogeneous, 3D nature of the convection (see bottom plots in Figures 3 and 4) below the stagnant lid, a strong linear diapir extends along the strike of the shear heating zone. The topography resulting from the shear heating remains linear along its length (see top plots in Figures 3 and 4). The linear ridge-like feature is mainly influenced by the distribution of shear heating. This supports the idea that shear heating can explain the highly linear nature of Europan ridges even in the presence of 3D heterogeneous convection.

4. Discussion

[15] Our simulated topography broadly resembles that of Europan ridges, including (in most simulations) the shallow marginal troughs on either side of the ridge, although the central trough is not reproduced. Explaining this feature may require mass drainage and the effects of elasticity and

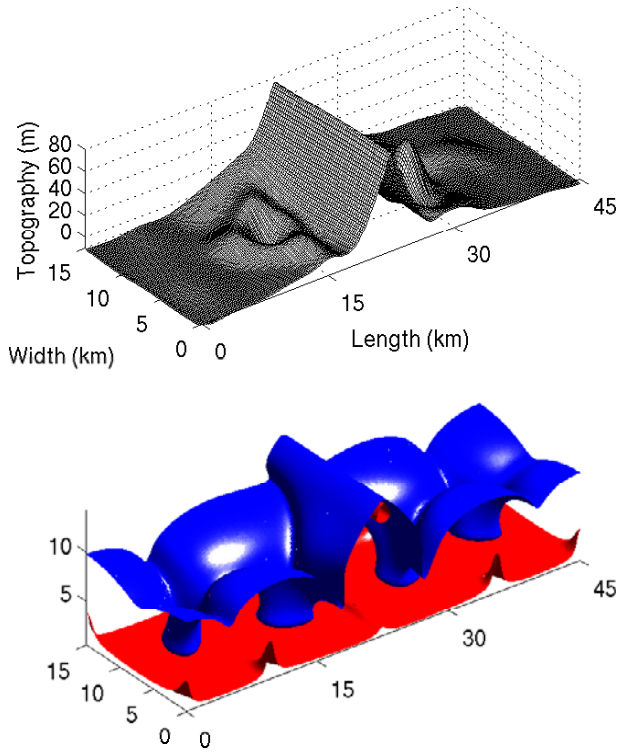

Figure 3. (top) Topography and (bottom) temperature from a 3D model in a domain 45 km long, 15 km deep, and 15 km wide. Red color shows the temperature isosurface at 257 K, and blue color shows the temperature isosurface at 216 K. The Rayleigh number is 1.8×10^6, activation energy for viscosity is 20 kJ/mol, and depth of shear heating is 3 km.

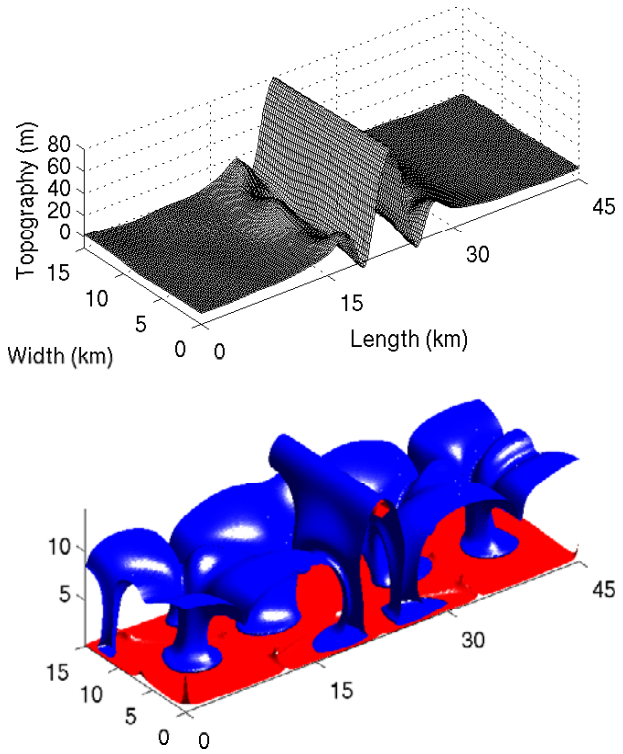

Figure 4. (top) Topography and (bottom) temperature from a 3D model in a domain 45 km long, 15 km deep, and 15 km wide. Red color shows the temperature isosurface at 257 K, and blue color shows the temperature isosurface at 216 K. The Rayleigh number is 1.8×10^7, the activation energy for viscosity is 20 kJ/mol, and depth of shear heating is 3 km.

flexure on the uplifted region, which are excluded here. Despite this deficiency, our simulations support the idea that shear heating, if strong enough, can produce Europa's ridges.

[16] The magnitude of shear heating along fractures remains uncertain. As previously discussed, *Nimmo and Gaidos* [2002] used a 2D diffusion model to estimate that temperature increases along the fault could reach ~60 K. In contrast, *Preblich et al.* [2007] performed finite-element calculations of tidal walking, and although they did not track the long-term thermal evolution, they estimated that only 3–5 K of heating would result from shear along fractures. The disagreement may result from the fact that the Preblich et al. model did not consider frictional fault heating, which is the dominant heat generation process in work by *Nimmo and Gaidos* [2002], nor did their estimate account for the positive feedback where modest initial temperature increases induce softening that strengthens the localization of strain below the fault, leading to greater heating rates as the runaway progresses. This suggests that the actual heating is greater than they estimated. On the other hand, the *Nimmo and Gaidos* [2002] model assumes that the shear velocity along the fault is constant (rather than oscillatory as would occur with tidal flexing on Europa), which might lead to an overestimate of the shear heating because it forces the full strain rate in the brittle layer to occur along the fault rather than partitioning between fault slip and distributed elastic deformation. Future work can shed additional light on the appropriate magnitude of shear heating for Europa.

[17] Although the simulations here assumed a pure-ice composition and pure viscous material, compositional effects and elasticity could play an important role in ridge formation. In our models, the topography (~100 m) results from thermal buoyancy associated with the warm region under the ridge, but some Europan ridges reach heights of ~300 m. Another difficulty is that in our models the ridge would disappear over a thermal diffusion timescale of $\sim 10^7$ years once the shear heating stopped. The existence of ridges with heights up to ~300 m suggests that ridge topography may result in part from compositional buoyancy. This is consistent with inferences for Europan pits, domes, and bands [*Nimmo et al.*, 2003; *Pappalardo and Barr*, 2004; *Han and Showman*, 2005]. Because salt diffuses much more slowly that heat, such compositional buoyancy would have very long lifetimes, and this could help explain the ubiquity of ancient ridges on Europa that presumably no longer experience frictional heating. Furthermore, dynamic topography can be sustained over long timescales when elasticity is included [*Dombard and McKinnon*, 2006]. Compositional effects and elasticity should be considered in future studies of ridge formation by shear heating.

[18] **Acknowledgments.** This work was supported by grant NNX06AC41G from NASA's Planetary Geology and Geophysics Research Program. PSI contribution #427.

References

Barr, A. C., R. T. Pappalardo, and S. J. Zhong (2004), Convective instability in ice I with non-Newtonian rheology: Application to the icy Galilean satellites, *J. Geophys. Res.*, *109*, E12008, doi:10.1029/2004JE002296.

Billings, S. E., and S. A. Kattenhorn (2005), The great thickness debate: Ice shell thickness models for Europa and comparisions with estimated based on flexure at ridges, *Icarus*, *177*, 397–412.

Dombard, A. J., and W. B. McKinnon (2006), Folding of Europa's icy lithosphere: An analysis of viscous-plastic buckling and subsequent topographic relaxation, *J. Struct. Geol.*, *28*, 2259–2269.

Gaidos, E. J., and F. Nimmo (2000), Tectonics and water on Europa, *Nature*, *405*, 637.

Goldsby, D. L., and D. L. Kohlstedt (2001), Superplastic deformation of ice: Experimental observations, *J. Geophys. Res.*, *106*, 11,017–11,030.

Greeley, R., et al. (2004), Geology of Europa, in *Jupiter: The Planet, Satellites, and Magnetosphere*, edited by F. Bagenal, T. E. Dowling, and W. B. McKinnon, pp. 329–362, Cambridge Univ. Press, New York.

Greenberg, R., et al. (1998), Tectonic processes on Europa: Tidal stresses, mechanical response, and visible features, *Icarus*, *135*, 64–78.

Han, L., and A. P. Showman (2005), Thermo-compositional convection in Europa's icy shell with salinity, *Geophys. Res. Lett.*, *32*, L20201, doi:10.1029/2005GL023979.

Head, J. W., and R. T. Pappalardo (1999), Morphological characteristics of ridges and triple bands from Galileo data (E4 and E6) and assessment of a linear diapirism model, *J. Geophys. Res.*, *104*, 24,223–24,236.

Kadel, S. D., S. A. Fagents, R. Greeley, and the Galileo SSI team (1998), Trough-bounding ridge pairs on Europa—Considerations for an endogenic model of formation, in *Lunar Planet. Sci.*, *XXIX*, abstract 1078.

King, S. D., A. Raefsky, and B. H. Hager (1990), ConMan: Vectorizing a finite element code for incompressible two-dimensional convection in the Earth's mantle, *Phys. Earth Planet. Inter.*, *59*, 195–207.

McKinnon, W. B. (1999), Convective instability in Europa's floating ice shell, *Geophys. Res. Lett.*, *26*, 951–954.

Melosh, H. J., and E. P. Turtle (2004), Ridges on Europa: Origin by incremental ice-wedging, *Lunar Planet. Sci.*, *XXXV*, abstract 2029.

Mitri, G., and A. P. Showman (2005), Convective-conductive transitions and sensitivity of a convecting ice shell to perturbations in heat flux and tidal heating rate: Implications for Europa, *Icarus*, *177*, 447–460.

Moresi, L., S. Zhong, and M. Gurnis (1996), The accuracy of finite element solutions of Stokes' flow with strongly varying viscosity, *Phys. Earth Planet. Inter.*, *97*, 83–94.

Nimmo, F., and E. Gaidos (2002), Strike-slip motion and double ridge formatioin on Europa, *J. Geophys. Res.*, *107*(E4), 5021, doi:10.1029/2000JE001476.

Nimmo, F., and M. Manga (2002), Causes, characteristics and consequences of convective diapirism on Europa, *Geophys. Res. Lett.*, *29*(23), 2109, doi:10.1029/2002GL015754.

Nimmo, F., R. T. Pappalardo, and B. Giese (2003), On the origins of band topography, Europa, *Icarus*, *166*, 21–32.

Pappalardo, R. T., and A. C. Barr (2004), The origin of domes on Europa: The role of thermally induced compositional diapirism, *Geophys. Res. Lett.*, *31*, L01701, doi:10.1029/2003GL019202.

Pappalardo, R. T., et al. (1999), Does Europa have a subsurface ocean? Evaluation of the geological evidence, *J. Geophys. Res.*, *104*, 24,015–24,055.

Preblich, B., R. Greenberg, J. Riley, and D. O'Brien (2007), Tidally driven strike-slip displacement on Europa: Viscoelastic modeling, *Planet. Space Sci.*, *55*, 1225–1245.

Showman, A. P., and L. Han (2004), Numerical simulations of convection in Europa's ice shell: Implications for surface features, *J. Geophys. Res.*, *109*, E01010, doi:10.1029/2003JE002103.

Showman, A. P., and L. Han (2005), Effects of plasticity on convection in an ice shell: Implications for Europa, *Icarus*, *177*, 425–437.

Sullivan, R., et al. (1998), Episodic plate separation and fracture infill on the surface of Europa, *Nature*, *391*, 371–373.

Tobie, G., G. Choblet, and C. Sotin (2003), Tidally heated convection: Constraints on Europa's ice shell thickness, *J. Geophys. Res.*, *108*(E11), 5124, doi:10.1029/2003JE002099.

Zhong, S., M. Gurnis, and L. Moresi (1998), Role of faults, nonlinear rheology, and viscosity structure in generating plates from instantaneous mantle flow models, *J. Geophys. Res.*, *103*, 15,255–15,268.

L. Han, Planetary Science Institute, 1700 East Fort Lowell, Suite 106, AZ 85719, USA. (han@psi.edu)

A. P. Showman, Department of Planetary Sciences, Lunar and Planetary Laboratory, University of Arizona, Tucson, AZ 85721, USA.